

Supplementary Information

Ion Accumulation Induced High Capacitance Supercapacitor Based on Micro-Porous Graphene

Bhaskar Pattanayak^{a,b}, Phuoc-Anh Le^c, Debashis Panda^{a,b}, Firman Mangasa Simanjuntak^d, Kung-Hwa Wei^c, Tan Winie^e, & Tseung-Yuen Tseng^{b,*}

^aDepartment of Electrical Engineering and Computer Science, National Yang Ming Chiao Tung University, Hsinchu City 30010, Taiwan

^bInstitute of Electronics, National Yang Ming Chiao Tung University, Hsinchu City 30010, Taiwan

^cDepartment of Material Science and Engineering, National Yang Ming Chiao Tung University, Hsinchu City 30010, Taiwan

^dCentre for Electronics Frontiers, University of Southampton, Southampton SO171BJ, United Kingdom

^eFaculty of Applied Sciences, Universiti Teknologi MARA, 40450, Shah Alam, Malaysia

*Email:- tseng@cc.nctu.edu.tw

Fabrication Process

Porous graphene was synthesized by the thermal annealing and copolymerization method. In a typical process, 1 g glucose and 0.5 g NH_4Cl were well mixed using mortar at room temperature, and resulted mixture was calcined at 950°C for 4.5 h in Argon atmosphere at a ramping rate of $4^\circ\text{C}/\text{min}$. The resulted material was crushed by mortar for further characterization.

Material Characterization-

The morphology of the grapheme was observed by Field Emission Scanning electron microscopy (FESEM) (Hitachi SU-8010) and high-resolution transmission electron microscope (TEM)(JEOL JEM-2010F). The crystallinity of the graphene was characterized by powder X ray diffraction(BRUKER D2 PHASER) with $\text{Cu K}\alpha$ radiation. Raman spectrometer (Jobin Yvon, Horiba) with Argon laser of 520 nm wavelength was used to observe defects and layer number of the graphene. The specific surface area was characterized by Brunauer-Emmett-Teller (BET) surface area analyzer (ASAP, 2020). The XPS (ULVAC-PHI Quantera SXM) was performed to examine composition of the graphene with Pt as a reference.

Preparation of Working Electrode and Supercapacitor

The working electrode of this study was prepared by mixing porous graphene, polyvinylidene fluoride (PVDF), and carbon black as active material, binder, and conductive material, respectively, in a weight ratio of 85: 10: 5 in N-methyl pyrrolidone (NMP) solution. The resulting homogeneous slurry was coated on the graphite sheets and dried at 80°C for 15 h in a vacuum.

To fabricate symmetrical solid-state supercapacitor, the gel polymer electrolyte was prepared at first. 1 g PVA and 10 ml of 1 M KOH were mixed and heated at 90°C to form a transparent

gel for the electrolyte. After cooling down to room temperature, two identical electrodes were submerged into the polymer gel electrolyte and dried overnight at room temperature. After that, two electrodes with gel polymer electrolyte coating were pressed together in a sandwich manner to fabricating symmetrical supercapacitor.

Electrochemical Characterization

For electrochemical performances, Autolab electrochemical analyzer was used to perform cyclic voltammetry (CV), galvanostatic charge/ discharge cycling (GCD), and electrochemical impedance spectroscopy (EIS) examinations. For electrochemical characterization of the graphene electrode, the three-electrode cell was configured by using porous graphene deposited on a graphite sheet, Ag/AgCl, and platinum as a working electrode, reference electrode, and counter electrode, respectively, in an aqueous KOH electrolyte solution with a varying concentration (0.1, 0.5, 1.0, 2.0, and 6.0 M).

Calculation of Specific Capacitance, Energy Density, and Power Density

The specific capacitance (C in $F\ g^{-1}$) is calculated from the result of cyclic voltammetry by using the equation

$$C = \frac{\int_{V_1}^{V_2} I(V)dV}{m\gamma\Delta V} \quad (1)$$

Where I , m , γ , and ΔV are current (A), active mass (g) loading, scan rate ($V\ s^{-1}$), and potential window (V).

The galvanostatic charge-discharge profile also provides specific capacitance by using the following equation

$$C = \frac{I\Delta t}{m\Delta V} \quad (2)$$

Where I represent discharge current in amp, Δt is the discharge time in sec for voltage window ΔV (volt) and m (g) is the active mass loading.

Energy density E (Wh kg^{-1}) and power density P (W kg^{-1}) are calculated by the equations

$$E = \frac{1}{(2 \times 3.6)} C \times (\Delta V)^2 \quad (3)$$

$$P = \frac{E}{\Delta t} \times 3600 \quad (4)$$

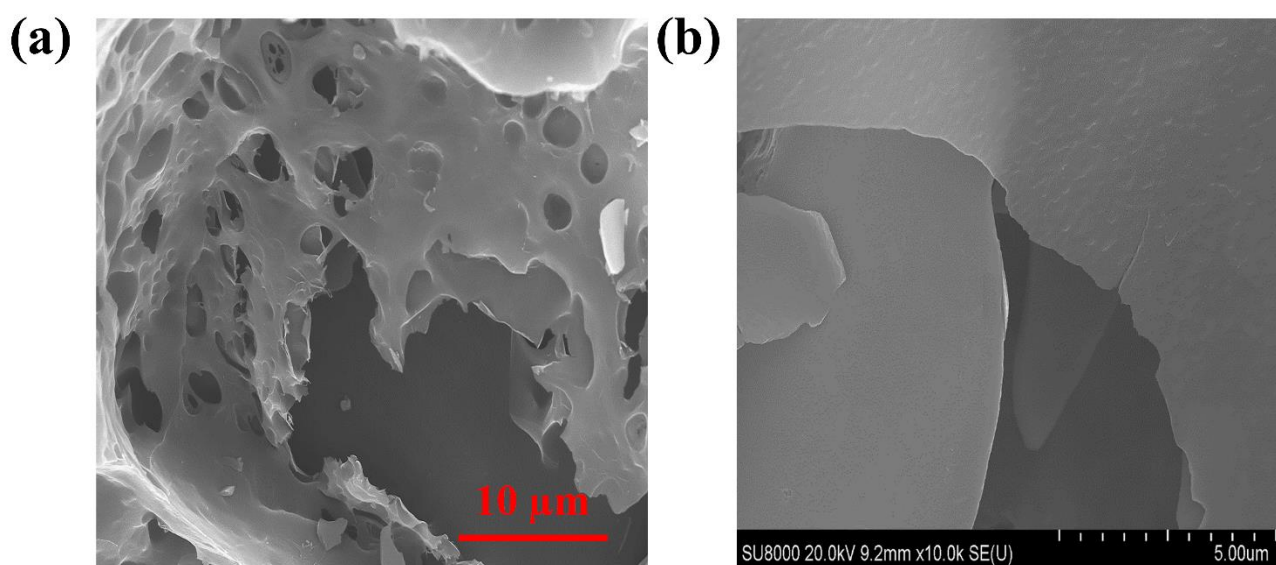


Figure S1 SEM images of porous graphene. (a) non-uniform distribution of individual graphene sheet edges. (b) Large graphene sheets are crumpled and overlapped with each other to creating macropores with large porosity.

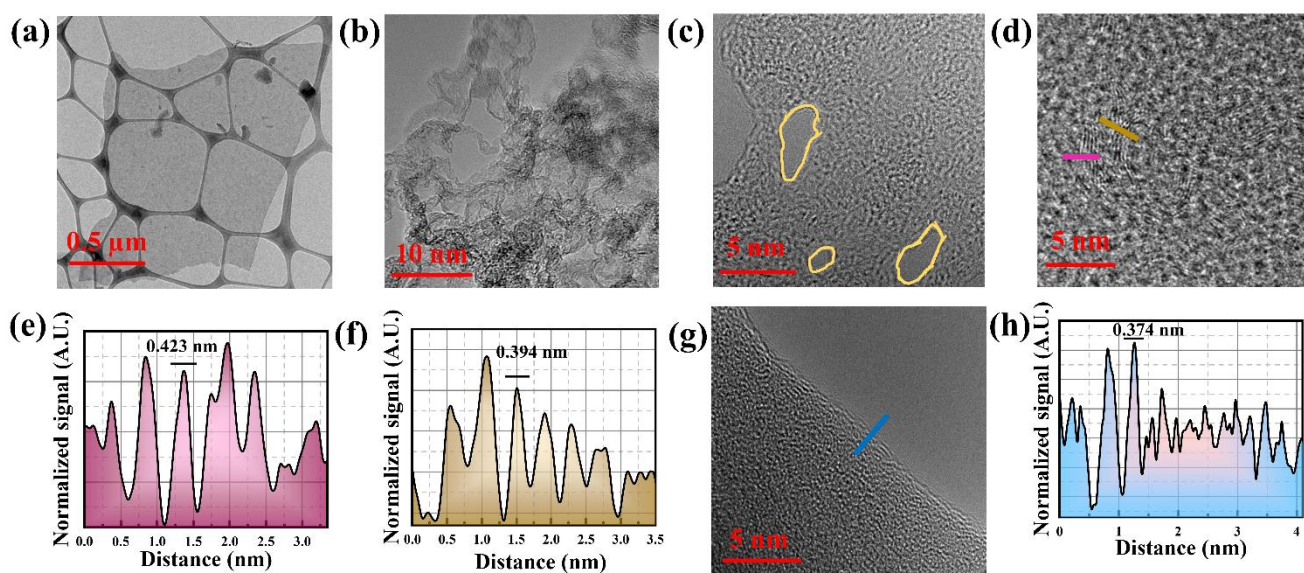


Figure S2 HRTEM images of (a) large-area graphene sheet, (b) concave like multilayer graphene, (c) non uniform pores in the graphene, and (d) concave like multilayer graphene edges. (e,f) line profiles of (d), two positions marked as a pink and yellow colour representing the interlayer spacing at different positions. (g) HRTEM image of graphene straight edges. (h) line profile of (g) representing the interlayer spacing.

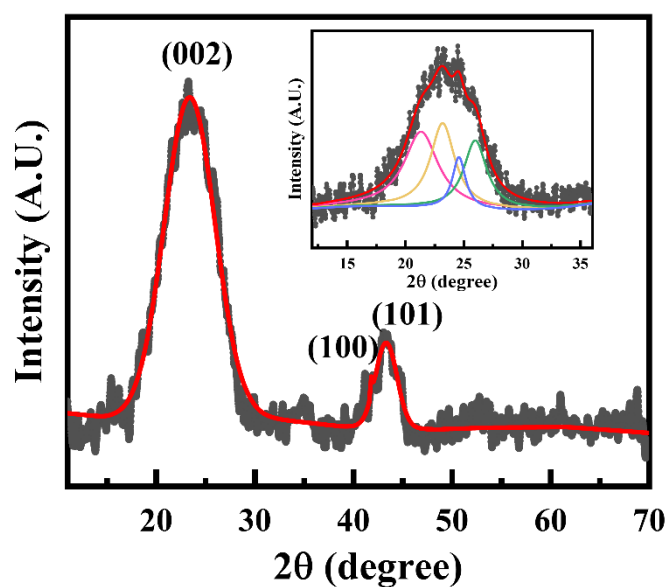


Figure S3 X-ray diffraction spectra of porous graphene. Inset showing multiple Lorentzian fitting in 2θ ranges from 19° to 30° .

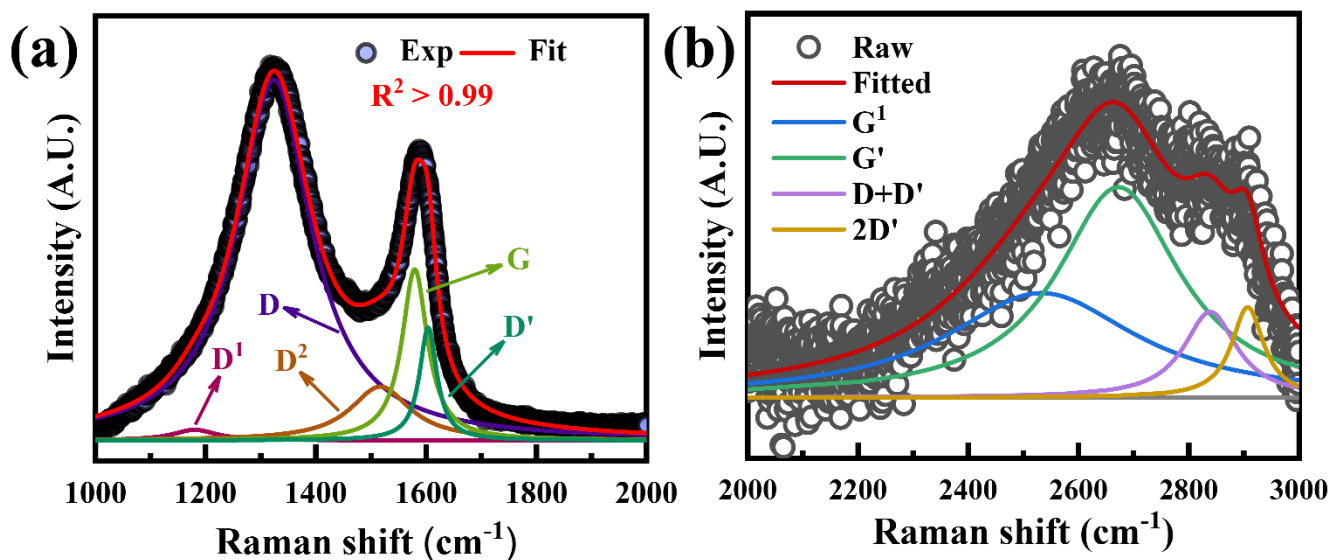


Figure S4 Raman spectra with multiple Lorentz fitting of (a) D and G band, (b) 2D band.

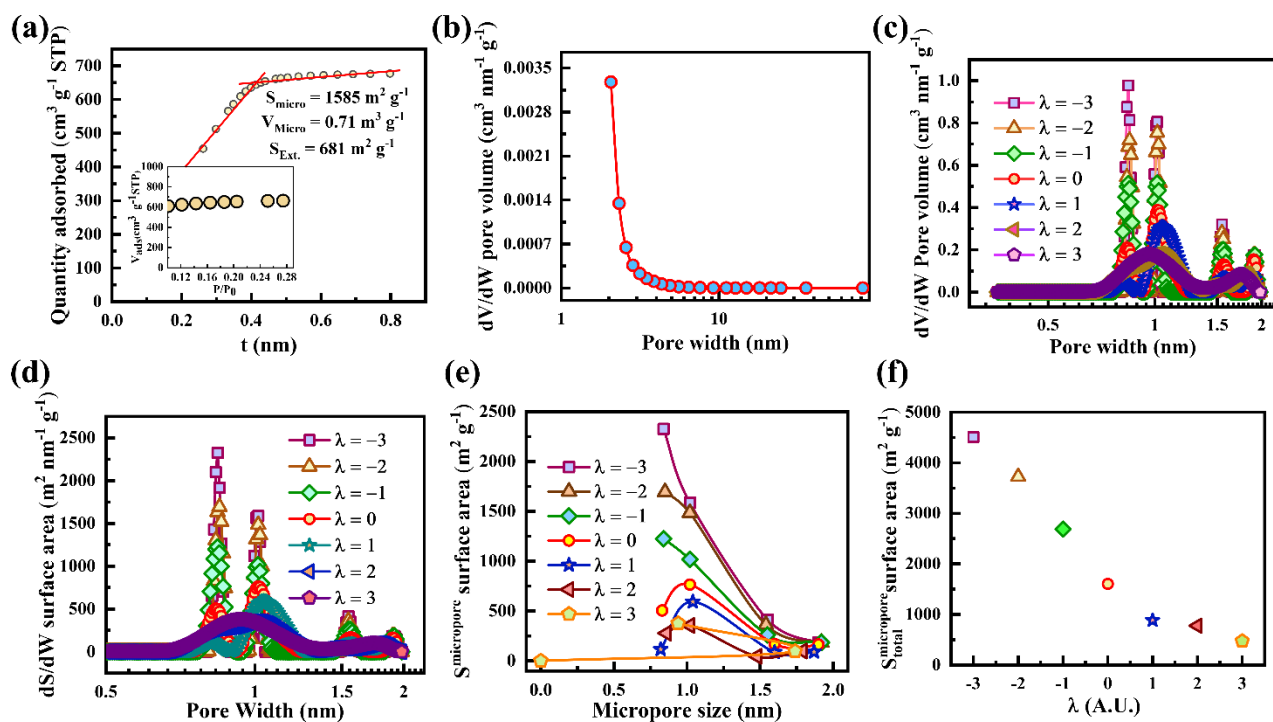


Figure S5 (a) t-plot method to calculate microporous and external surface area and (inset) corresponding N₂ adsorption-desorption isotherm in which the microporous surface area calculated. (b) BJH pore size distribution. (c) NLDFT Pore size distribution at a various regularizing parameter λ varies from -3 to 3. Variation of (d) dS/dW and (e) microporous surface area associated with different micropore size, at different λ . (f) variation of total microporous surface area with λ . Total microporous surface area calculated from NLDFT method ($S_{\text{micropore}}^{\text{total}}$) is consistent with classical t-plot method (S_{micro}). Therefore, $\lambda = 0$, provides the better result.

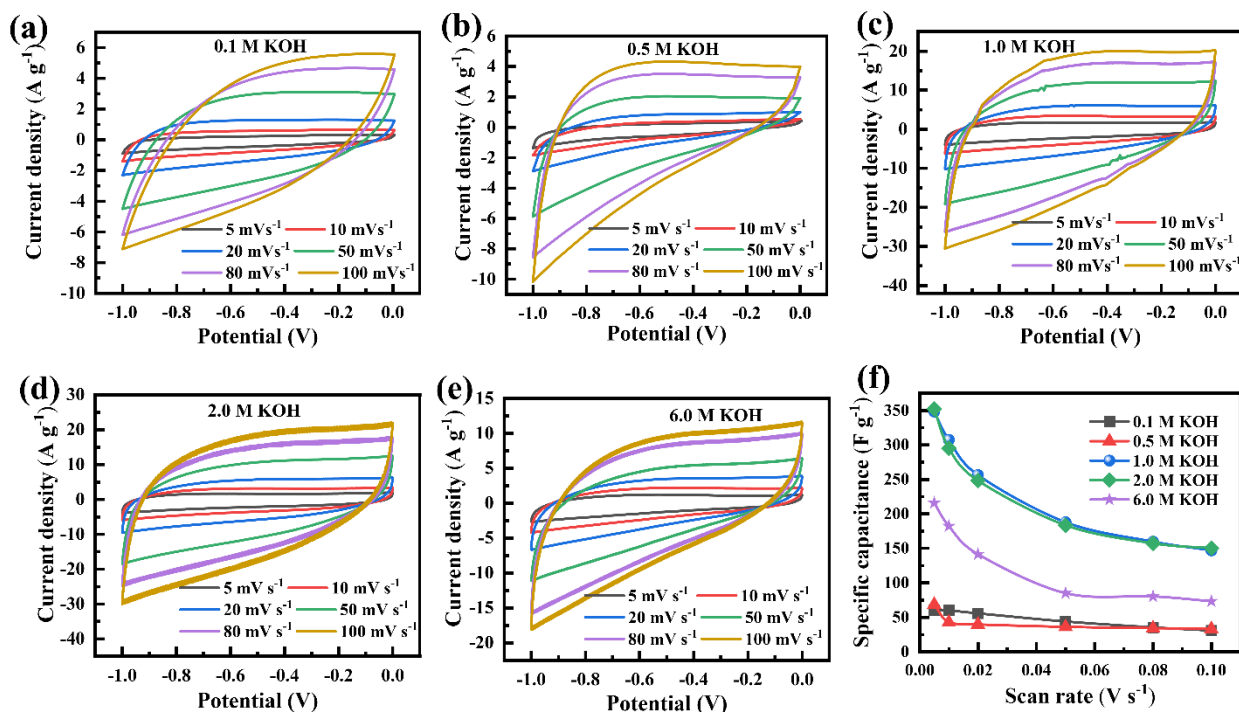


Figure S6 (a-e) Cyclic voltammetry response of porous graphene with various electrolyte concentrations at different scan rates. (f) Variation of specific capacitance with scan rate using equation 1.

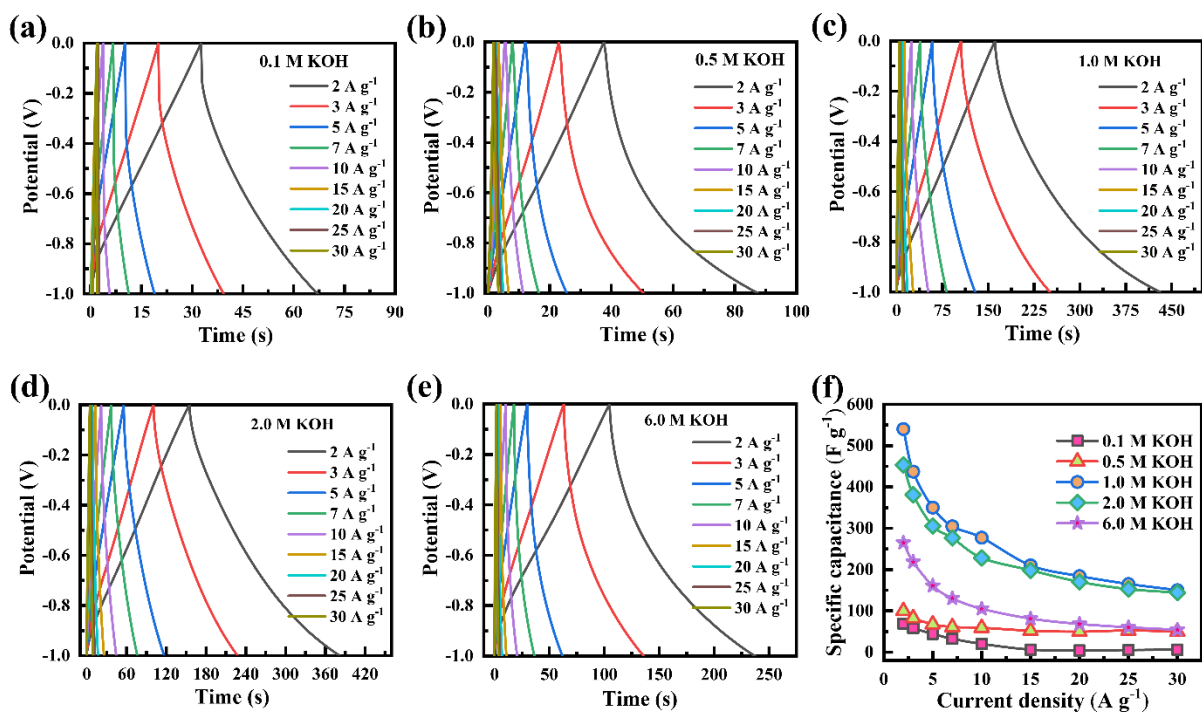


Figure S7 (a-e) Galvanostatic charge discharge response of porous graphene with varying electrolyte concentrations at different current densities. (f) Variation of specific capacitance with current density using equation 2.

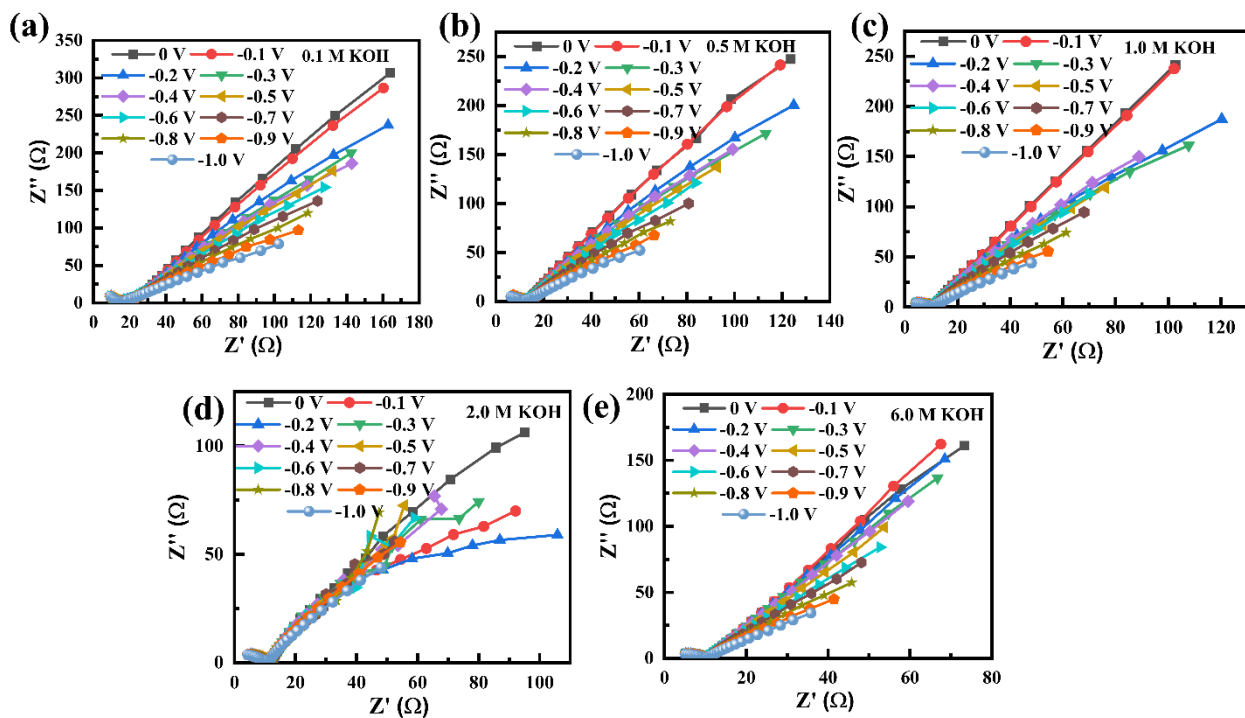


Figure S8 (a-e) EIS characteristics at different potential ranging from 0 to -1.0 V with concentrated electrolytes.

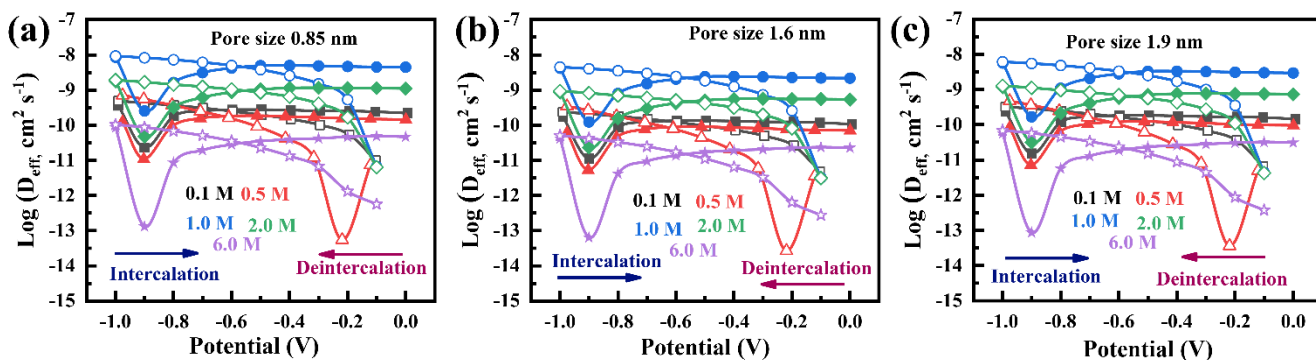


Figure S9 Variation of effective diffusion coefficient with potential during intercalation and deintercalation processes for different electrolyte concentration for the pore sizes of (a) 0.85 nm, (b) 1.6 nm and (c) 1.9 nm, respectively.

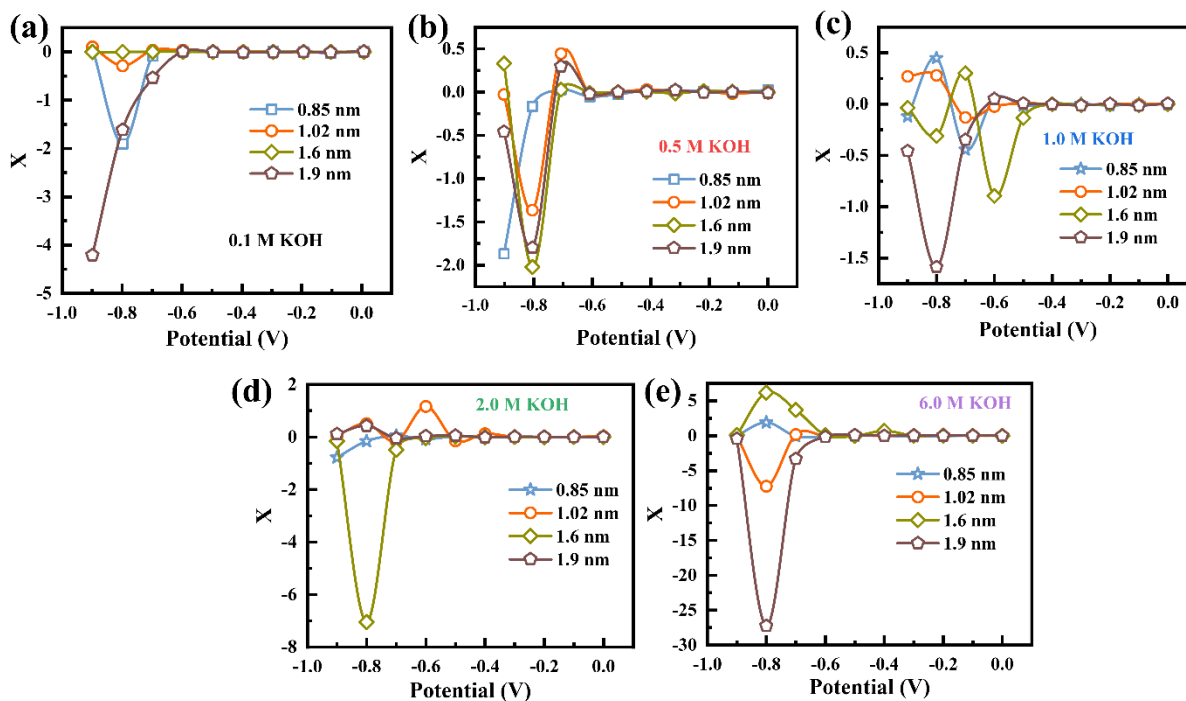


Figure S10 Variation of charge storage parameter X with potential for the electrode with different pore sizes (indicated) in (a) 0.1 M (b) 0.5 M (c) 1 M (d) 2 M and (e) 6 M KOH concentrations.

Supplementary Note 1

Crystallite size and defect density calculation-

Crystallite size (L_a) and defect density from Raman spectra can be calculated by using the following equations¹

Crystallite size (L_a):

$$L_a = (2.4 \times 10^{-10}) \lambda_{laser}^4 (nm) \left(\frac{I_D}{I_G} \right)^{-1} \quad (5)$$

Where $\lambda_{laser} = 514 \text{ nm}$

I_D/I_G = integrated area ratio of D and G band

$I_D/I_G = 5.59 - 6.99$

$L_a = 3 \text{ nm}$ for $I_D/I_G = 5.59$

$L_a = 2.4 \text{ nm}$ for $I_D/I_G = 6.99$

Defect density (N_D) :

$$N_D (cm^{-2}) = \frac{(1.8 \pm 0.5) \times 10^{22}}{\lambda_{laser}^4 (nm)} \times \frac{I_D}{I_G} \quad (6)$$

$N_D (cm^{-2}) = 1.44 \times 10^{12}$ for $I_D/I_G = 5.59$

$N_D (cm^{-2}) = 1.8 \times 10^{12}$ for $I_D/I_G = 6.99$

Supplementary Note 2

Pore size distribution from NLDFT calculation

Based on the nonlocal density functional theory (NLDFT), the equation for calculating pore size distribution is^{2,3,4}

$$N_{\text{exp}}\left(\frac{P}{P_0}\right) = \int_{D_{\text{min}}}^{D_{\text{max}}} N_{\text{NLDFT}}\left(\frac{P}{P_0}, D\right) \text{PSD}(D) dD + \lambda \int_{D_{\text{min}}}^{D_{\text{max}}} [\text{PSD}'(D)]^2 dD \quad (7)$$

Where D = Pore diameter

$\text{PSD}(D)$ = Pore size distribution

λ = Regularizing parameter to accurate pore size distribution based on the NLDFT

N_{NLDFT} = Theoretical N_2 adsorption

N_{exp} = experimental N_2 adsorption isotherm at 77K

P/P_0 = Relative pressure.

To calculate accurate pore size distribution, we varied the λ from -3 to 3. As in the Fig. S5 (c, d), when $\lambda = 3$, the pore volume (dV/dW) as well as the surface area (dS/dW) become broader. Further decreasing λ (upto -3), dV/dW and dS/dW become sharper. The NLDFT calculated micropore surface area ($S^{\text{micropore}}_{\text{total}}$) should be conformable with classically calculated micropore surface area (S_{micro}). Therefore, regularizing parameter $\lambda = 0$ provides better result. The calculated values are provided in Table 1. The optimized values are also marked in the Table 1.

Table 1:-**Pore size and corresponding microporous surface area calculated by NLDFT**

λ	Pore size (nm)	Surface area ($\text{m}^2 \text{ nm}^{-1} \text{ g}^{-1}$)	Pore volume ($\text{cm}^3 \text{ nm}^{-1} \text{ g}^{-1}$)	Total surface area ($\text{m}^2 \text{ nm}^{-1}$ g^{-1})
-3	0.84	2324.6	0.98	4508.5
	1.02	1585.7	0.81	
	1.55	415	0.32	
	1.9	183.2	0.17	
-2	0.85	1693.2	0.72	3723.1
	1.02	1484	0.75	
	1.54	362.3	0.28	
	1.92	183.6	0.18	
-1	0.84	1224.4	0.52	2687.6
	1.02	1017.8	0.52	
	1.55	260.6	0.20	
	1.92	184.6	0.17	
0	0.85	505.2	0.21	1603.1
	1.02	765.2	0.39	
	1.6	168.7	0.13	
	1.9	164	0.16	
1	0.82	115.9	0.05	883.8
	1.04	591.8	0.31	
	1.6	56.2	0.07	
	1.87	89.9	0.08	
2	0.86	277.6	0.12	776.1
	1.02	354.7	0.18	
	1.48	45.1	0.03	
	1.79	98.7	0.09	
3	0.94	375.3	0.18	472.2
	1.74	96.9	0.08	

Table 2**Comparison of the properties of recently published porous carbon based electrodes with those of this work**

Material structure	BET surface area (m² g⁻¹)	Electrolyte	Specific capacitance (F g⁻¹)	Capacitance retention	References
GO/NC	1493	6 M KOH	405.6	95.8% @ 5000 cycles	5
PVA/rGO/PVP	1215	3 M KCl	223	82.3 @10000 cycles	6
a-rCGO	2428.6	6 M KOH	225	92.1% @ 10000 cycles	7
DDLGC/GO ₈	893.9	6 M KOH	366	99.9% @10000 cycles	8
NG film	351.43	EMIMBF ₄	196.7	78.3% @ 5500 cycles	9
Porous graphene@ Mn ₃ O ₄	1327	1 M Na ₂ SO ₄	208.3	86% @2000 cycles	10
Porous graphene/carbon	1074	6 M KOH	341	91.8% @ 5000 cycles	11
NPC-3DG	726.9	1 M H ₂ SO ₄	530	-	12
Porous Graphene	2266	1 M KOH	540	~100 % @ 7000 cycle	This work

References -

- 1 A. C. Ferrari, *Solid State Commun.*, 2007, **143**, 47–57.
- 2 A. J. Lecloux, R. Atluri, Y. V. Kolen'ko and F. L. Deepak, *Nanoscale*, 2017, **9**, 14952–14966.
- 3 A. Galarneau, F. Villemot, J. Rodriguez, F. Fajula and B. Coasne, *Langmuir*, 2014, **30**, 13266–13274.
- 4 G. Kupgan, T. P. Liyana-Arachchi and C. M. Colina, *Langmuir*, 2017, **33**, 11138–11145.
- 5 L. Wan, C. Du and S. Yang, *Electrochim. Acta*, 2017, **251**, 12–24.
- 6 D. T. Bakhoun, K. O. Oyedotun, S. Sarr, N. F. Sylla, V. M. Maphiri, N. M. Ndiaye, B. D. Ngom and N. Manyala, *J. Energy Storage*, 2022, **51**, 104476.
- 7 L. Sun, Z. Zhao, Y. Sun, X. Wang, X. Liu, Y. Yang and J. Qiu, *Diam. Relat. Mater.*, 2020, **106**, 107827.
- 8 M. Xu, A. Wang, Y. Xiang and J. Niu, *J. Clean. Prod.*, 2021, **315**, 128110.
- 9 Y. Chen, Y. Jiang, Z. Liu, L. Yang, Q. Du and K. Zhuo, *Electrochim. Acta*, 2021, **366**, 137414.
- 10 T. Wang, Q. Le, X. Guo, M. Huang, X. Liu, F. Dong, J. Zhang and Y. X. Zhang, *ACS Sustain. Chem. Eng.*, 2019, **7**, 831–837.
- 11 Q. Li, M. Hu, K. Wang and X. Wang, *Catal. Today*, 2019, **330**, 228–239.
- 12 X. Zhang, X. Gao, Z. Wu, M. Zhu, Q. Jiang, S. Zhou, Y. Huang and Z. Rao, *Ionics (Kiel)*, 2019, **25**, 6017–6023.